Paper No.
6126

NACE INTERNATIONAL CORROSION 2015 CONFERENCE & EXPO

Repassivation Behavior Of UNS N06022 In Chloride-Containing Solutions

Hundal Jung
Center for Nuclear Waste Regulatory Analyses
6220 Culebra Road
San Antonio, TX 78238
USA

Tae M. Ahn
U.S. Nuclear Regulatory Commission
MS E2–B2
Washington, DC 20555-0001
USA

ABSTRACT

This paper evaluates a potential degradation process due to sulfur segregation that might occur on UNS N06022 waste package material in a geologic repository setting. To evaluate susceptibility to sulfur-enhanced corrosion, the repassivation behavior of UNS N06022 was investigated in sulfur-containing chloride solutions using a scratch technique. Once the passive film was disrupted by scratching, anodic current increased abruptly to the peak current and thereafter decreased. With increasing potential, peak current increased and thickness of the reformed passive film increased. The addition of 0.01 M Na_2S yielded nearly identical results as the sulfur-free cases. In simulated concentrated water containing 0.01 M Na_2S, repassivation commenced immediately after scratching. However, an increase of the concentration to 0.1 M Na_2S at 22 °C or increase of temperature to 60 °C causes a decrease in peak current. Results indicated that UNS N06022 can repassivate in a relatively short period in sulfur-containing solutions.

Key words: repassivation, UNS N06022, sulfur contamination

INTRODUCTION

Passivity in metals and alloys is generally a result of a thin, protective oxide film on the metal surface that efficiently inhibits corrosion.[1] UNS N06022 which is a nickel based chromium and molybdenum containing alloy, a potential waste package material for disposing radioactive waste, is a passive metal and typically shows high resistance to various modes of corrosion including general corrosion, localized corrosion, and stress corrosion cracking (SCC) in a wide range of environmental conditions.[2-4] The high corrosion resistance of this alloy is due to the formation of a thin,

chromium-enriched passive oxide film on the alloy surface.[4,5] In the absence of environmental conditions leading to localized corrosion or SCC, this alloy is expected to corrode uniformly with very low corrosion rates in aqueous environments.[6]

In the case of deterioration or loss of passivity (i.e., depassivation) under certain conditions, however, the corrosion rate could substantially increase by active dissolution or localized corrosion (e.g., pitting). This may result in a shorter service lifetime of this alloy. Therefore, if there is an event causing film instability and film breakdown, the repassivation behavior of this alloy could control the extent of the corrosion damage. One potential mechanism for film breakdown is sulfur-induced localized corrosion followed by active dissolution. Sulfur, present either in an aqueous environment or alloyed in the metal matrix as an impurity has been widely recognized to detrimentally affect the passivation of various metals and alloys. In particular, Marcus and coauthors have reported detailed studies on the effects of sulfur on the corrosion behaviors of nickel, nickel-based alloys including nickel-iron, nickel–chromium or nickel–chromium–iron, nickel–molybdenum, and iron-17% chromium-14.5% nickel-2.3% molybednum stainless steel using electrochemical, radiotracer, and surface analysis techniques.[7-15] These studies showed enhanced localized corrosion susceptibility (i.e. pitting corrosion) due to segregated sulfur adsorbed from the aqueous solution or originated in the alloy at test temperatures between the room temperature (22°C) and about 200°C. Marcus, et al. proposed that sulfur segregated on the metal surface inhibits a formation of protective passive film and could also lead to passive film breakdown.[7-11] On the other hand, Marcus, et al. also reported the beneficial role of alloyed chromium and molybdenum in passivation of nickel-based alloys by counteracting detrimental effects of sulfur.[12-15]

In the presence of sulfur, the corrosion resistance of these passive alloys can be measured by the repassivation capability of the alloys in solutions containing sulfur species. In this study, the scratch repassivation technique was designed to measure the repassivation kinetics of UNS N06022 when the surface was mechanically damaged by scratching. The electrical current versus time transient after scratching was monitored, and the resultant current changes were compared at different sulfur concentrations (i.e., 0, 0.01, and 0.1 M Na_2S) in 0.5 M NaCl at two different temperatures (i.e., 22 °C and 60 °C). This study presents repassivation test results and discusses potential beneficial roles of chromium and molybdenum in the corrosion resistance of UNS N06022 in the presence of sulfur.

EXPERIMENTAL PROCEDURE

Materials

The working electrodes for the scratch tests were cylindrical UNS N06022 samples machined from a thick plate of UNS N06022. The samples had a 12.08-mm diameter and a 10.16-mm height. The samples were grounded to a 600-grit finish, cleaned with ethanol, and dried. The chemical composition of mill-annealed UNS N06022 (HT 2277–3–3266) is shown in Table 1.

Table 1
Chemical Composition of Mill-Annealed UNS N06022 (in Weight Percent)

Ni*	Cr*	Mo*	W*	Fe*	Co*	Si*	Mn*	V*	P*	S*	C*
Bal†	22.15	12.90	2.81	3.82	1.37	0.01	0.30	0.15	0.012	0.002	0.004
*Ni—nitrogen; Cr—chromium; Mo—molybdenum; W—tungsten; Fe—iron; Co—cobalt; Si—silicon; Mn—manganese; V—vanadium; P—phosphorous; S—sulfur; C—carbon †Bal—balance											

Test Solutions

Two different types of test solutions (0.5 M NaCl and simulated concentrated water; see Table 2) containing 0, 0.01, or 0.1 M Na_2S were prepared from analytical-grade chemicals and deionized water.

Table 2
Chemical Composition of Simulated Concentrated Water in This Study

Ion	K^+	Na^+	Mg^{2+}	Ca^{2+}	F^-	Cl^-	NO_3^-	SO_4^{2-}	HCO_3^-
mg/L	3,400	40,900	< 1	< 1	1,400	6,700	6,400	16,700	70,000

The initial pH of 0.5 M NaCl solutions without sulfur addition was approximately 6.7, while the initial pH of 0.5 M NaCl solutions with sulfur addition was approximately 10. The 0.5 M NaCl solutions containing 0.01 and 0.1 M Na_2S were adjusted to an initial pH of 7 with dilute HCl solution. The test solution was either deaerated by purging with purified N_2 gas (99.999 percent) for 30 minutes before and during the test or aerated by opening to air. The tests were conducted at solution temperatures of 22 and 60 °C. The fabrication material of the test cell permitted a maximum experimental temperature of only 60°C.

Test Procedures

Figure 1 shows an experimental setup for conducting a scratch repassivation test for UNS N06022. A cell was devised to measure the repassivation current of UNS N06022 working electrode samples after a surface scratch as shown in Figure 1. The samples were allowed to reach a pseudo-steady-state passive current, which usually required roughly 300 seconds. The scratch was made by impinging a diamond tip loaded on a stainless steel rod into a rotating working electrode surface for 1 second. For reproducibility, at least two scratches were made on one sample at two different locations along the sample surface by shifting the sample vertically at each test. The rapid reaction of a newly generated bare surface was observed as a current change. During the tests, the samples were rotated with a speed of 60 rpm. The average sizes of the scratched surface were 24 ± 3 μm wide, 20 ± 4 μm deep, and 3.79 cm long (i.e., the circular length of the working electrode), giving an average scratched area of about 1.75×10^{-2} cm^2. The potentials were measured against a saturated calomel reference (SCE) electrode. A platinum mesh was used as a counter electrode.

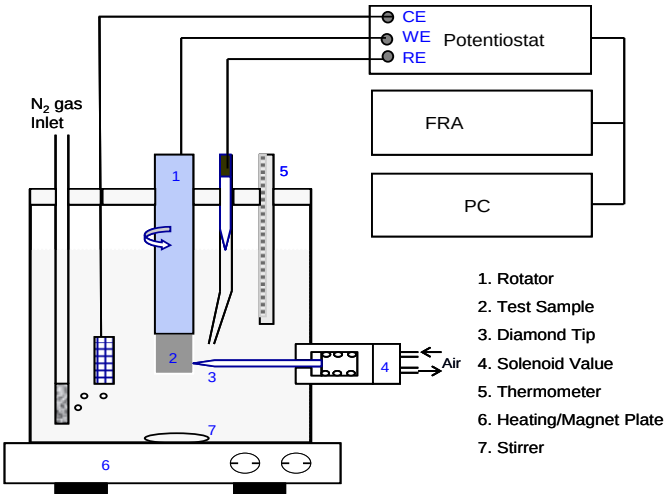

Figure 1: Schematics of the experimental setup for scratch repassivation test.

RESULTS AND DISCUSSIONS

Repassivation Behaviors of UNS N06022 at 22 °C

Effects of Applied Potential

Figures 2, 3, and 4 show the current versus time transient curves for the test samples when two successive scratches were made on the surface of the rotating working electrode at applied potentials of –0.1, 0.0, 0.2, and 0.5 V_{SCE} in deaerated 0.5 M NaCl solutions without sulfur addition and with a 0.01 and 0.1 M Na_2S addition, respectively, at 22 °C. The values of the peak currents are listed in Table 3. In Table 3, the peak current densities were corrected to disregard the current's contribution from the surrounding oxide film by subtracting the current density before scratching from the measured current density.

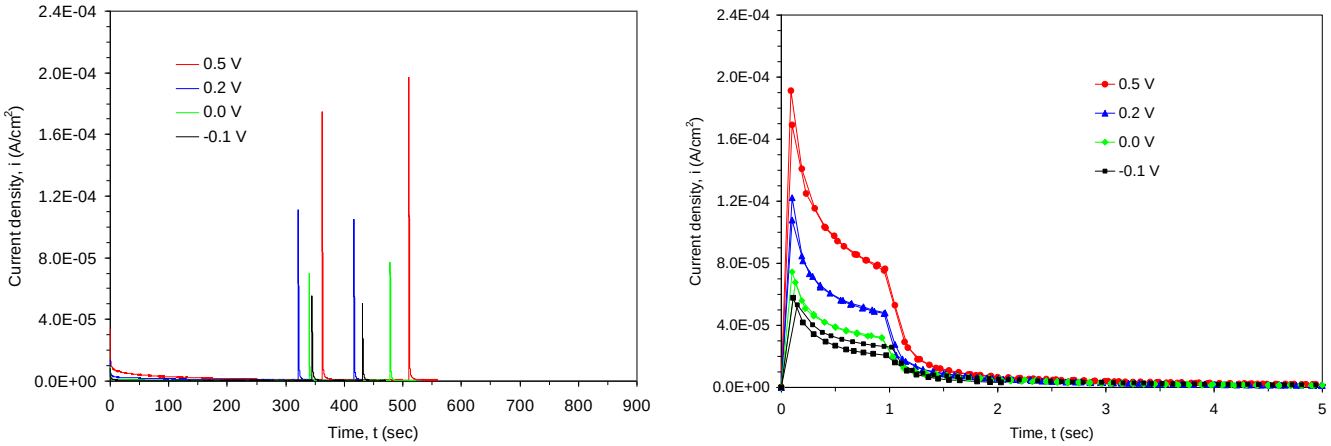

Figure 2: Potentiostatic polarization curves (a) and corrected current versus time transient curves (b) at various potentials in 0.5 M NaCl solution without sulfur at 22 °C.

Table 3
Peak Current Density Measured at −0.1, 0.0, 0.2, and 0.5 V_{SCE} in 0.5 M NaCl Solution Containing 0, 0.01, and 0.1 M Na_2S at 22 °C

Potential (V_{SCE})	Corrected i_{peak} (A/cm^2)							
	Without Sulfur		0.01 M Na_2S		0.1 M Na_2S		Average Ratio (0.01 M Sulfur Versus Without Sulfur)	Average Ratio (0.1M Sulfur Versus Without Sulfur)
	Peak #1	Peak #2	Peak #1	Peak #2	Peak #1	Peak #2		
−0.1	5.32×10^{-5}	5.78×10^{-5}	4.89×10^{-5}	5.78×10^{-5}	-1.73×10^{-5}	—	0.96	—
0.0	6.77×10^{-5}	7.45×10^{-5}	6.60×10^{-5}	7.89×10^{-5}	—	—	1.02	—
0.2	1.08×10^{-4}	1.22×10^{-4}	1.29×10^{-4}	1.00×10^{-4}	4.13×10^{-5}	4.44×10^{-5}	1.00	0.37
0.5	1.69×10^{-4}	1.91×10^{-4}	2.11×10^{-4}	1.52×10^{-4}	6.45×10^{-5}	7.97×10^{-5}	1.01	0.40

For all the tested samples, once a passive film was mechanically disrupted by scratching, the anodic current increased abruptly to the peak current and thereafter decreased as repassivation occurred.

The anodic current measured during repassivation can be presumed to be produced by two anodic processes: the metal dissolution reaction and the repassivation of oxide film. According to Burstein and Marshall, the anodic currents associated with metal dissolution for Type 304L SS in chloride solutions are negligibly small, except if metal dissolution is dominated by pitting.[16] Thus, it is reasonable that the anodic charge flowing from a newly generated metal surface of the tested samples in the present study can be exclusively due to passive film reformation because there was no observation of active dissolution of this alloy after scratching.

Without sulfur addition, the peak current increased proportionally as the anodic potential increased from −0.1 to 0.5 V_{SCE} as shown in Figure 2. The increase of peak current with increasing anodic potential was also observed for several iron based alloys such as Fe–18.5% Cr in 0.1 M H_2SO_4, Fe–18.8% Cr and Fe–18.6% Cr–2.5% Mo in 4 M HCl, and Type 304 SS in various solutions.[16-18] According to a model for repassivation kinetics of passive metals, Gilbert, et al. proposed the peak current increases as the reformed film thickness increases when film growth is the dominant process during repassivation.[19] Therefore, the film thickness is expected to increase as the applied potential increases from −0.1 to 0.5 V_{SCE} in the present study if the theory by Gilbert, et al. is applicable to this alloy.[19]

The charge transfer measured from the metal can be directly related to the scratched surface area. By neglecting the current associated with metal dissolution as previously mentioned, the amount of charge needed to form a passive film of a certain thickness can be estimated by using Faraday's law

$$q_{film} = \frac{\delta \rho z F A}{M_w} \quad (1)$$

where

q_{film} — film charge (Coulomb/cm^2)
δ — film thickness (cm)
ρ — film density (g/cm^3)
M_W — film molecular weight (g/mol)
z — number of electrons per cation
F — Faraday constant (96,485 Coulomb/mol)
A — scratched surface area (cm^2)

The repassivating charge is the area under the curve of the transient current response [i(t) versus t] after return to the steady state.

Using Equation 1, the thickness of the passive film that reformed on the UNS N06022 surface during repassivation was estimated. Considering chromium oxide (Cr_2O_3) and nickel oxide (NiO) are the main oxides, it was assumed that the film was composed of 50 percent Cr_2O_3 and 50 percent NiO by volume. The bare surface area was 1.75×10^{-2} cm^2; the calculated thickness of the passive film ranged from 1.8 nm at −0.1 V_{SCE} to 2.7 nm at 0.5 V_{SCE}. In the calculation, parameter values for Cr_2O_3 are z = 3, M_w = 151.9 g/mol, and ρ = 5.21 g/cm^3 and for NiO are Z = 2, M_w = 74.7 g/mol, and ρ = 6.67 g/cm^3.[20] Lloyd, et al.[21] observed similar ranges of passive film thickness formed on UNS N06022 when polarized in 1 M NaCl with 0.1 M H_2SO_4 at 85 °C. Using x-ray photoelectron spectroscopy and an ion-time secondary ion mass spectrometer, Lloyd, et al.[21] estimated the film thicknesses were 2 nm at 200 mV_{SCE} and 2.8 nm at 700 mV_{SCE} and the passive film consisted of a mixture of mainly chromium oxide (i.e., Cr_2O_3) and NiO. The increase of film thickness with the potential and the thickness estimates derived from the present study are consistent with the results from Lloyd, et al.[21]

The thickening of the passive film on a bare surface is associated with a decrease in current density with time, $i(t)$, according to a power law

$$i(t) = ct^{-n} \quad (2)$$

where

c and *n* — constants with given values for given metal/environments

A high *n* value represents a high repassivation rate. This equation is generally valid for the passivation of the passive alloys such as stainless steel and UNS N06022 under potentiostatic control. Because both alloys (i.e., stainless steel and UNS N06022) are the materials showing typically a strong passivation, it is reasonable to compare *n* values of these alloys with each other. A value of $n = 1$ was obtained for Type 304L SS in chloride solutions if the superimposed dissolution rate of the passive film was negligibly low.[22] If the dissolution rate of the passive film is not negligible, then, $n < 1$ (e.g., for iron in acid solution, $n = 0.7$).[22] From the present data of current versus time transient curves, the *n* values were determined from the slopes of the log *i*(*t*) versus log *t* plots after 1 second scratching according to Equation (2). At 0.5 V_{SCE}, *n* equaled 2, whereas at −0.1 V_{SCE}, *n* was 1.8. Compared to the stainless steel with its mean value of 1.04 in 1 M KOH, the higher values for UNS N06022 (1.8 to 2) indicate an increased capacity of UNS N06022 to repassivate.[16]

Effects of Sulfur Addition

Figure 3 presents the effects of sulfur addition on the repassivation behavior of UNS N06022. The addition of 0.01 M Na_2S yielded nearly identical results as the sulfur-free cases.

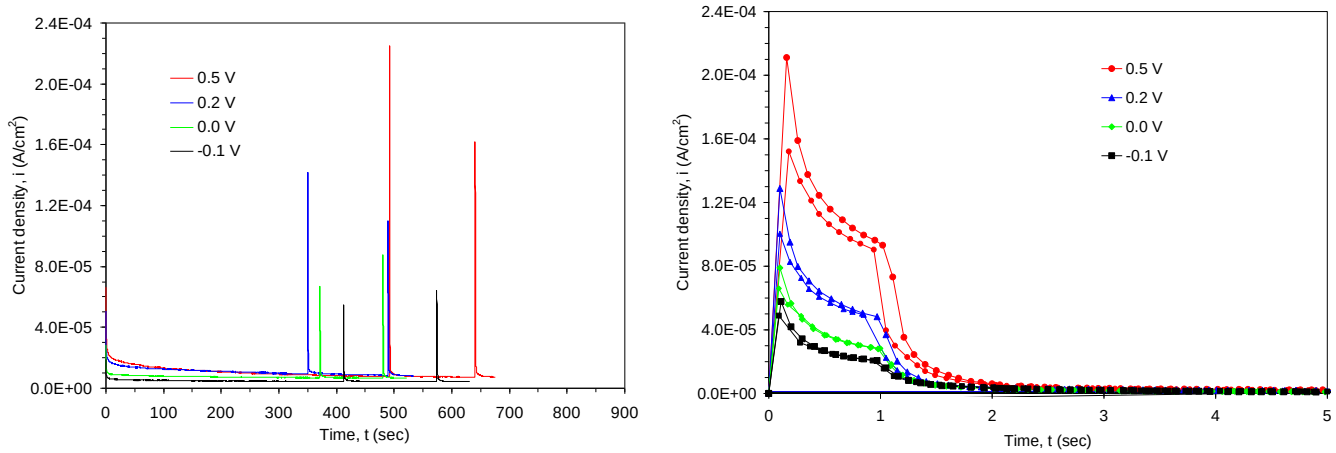

Figure 3: Potentiostatic polarization curves (a) and corrected current versus time transient curves (b) at various potentials in 0.5 M NaCl solution with 0.01 M Na_2S at 22 °C.

The current after scratching returned to the passive-state level quickly. The ratios of the peak current for the 0.01 M Na_2S cases to the peak current for cases without sulfur were roughly 1 (see Table 3). In addition, the *n* values for 0.01 M Na_2S cases also ranged from 1.8 at −0.1 V_{SCE} to 2 at 0.5 V_{SCE}. It could be inferred that the reformed film thickness for the 0.01 M Na_2S case was the same as the sulfur-free test. Therefore, it can be concluded that the repassivation capability of UNS N06022 does not deteriorate with addition of 0.01 M Na_2S. When the concentration of sulfur species increased to 0.1 M Na_2S, the peak current apparently decreased, as seen in Figure 4.

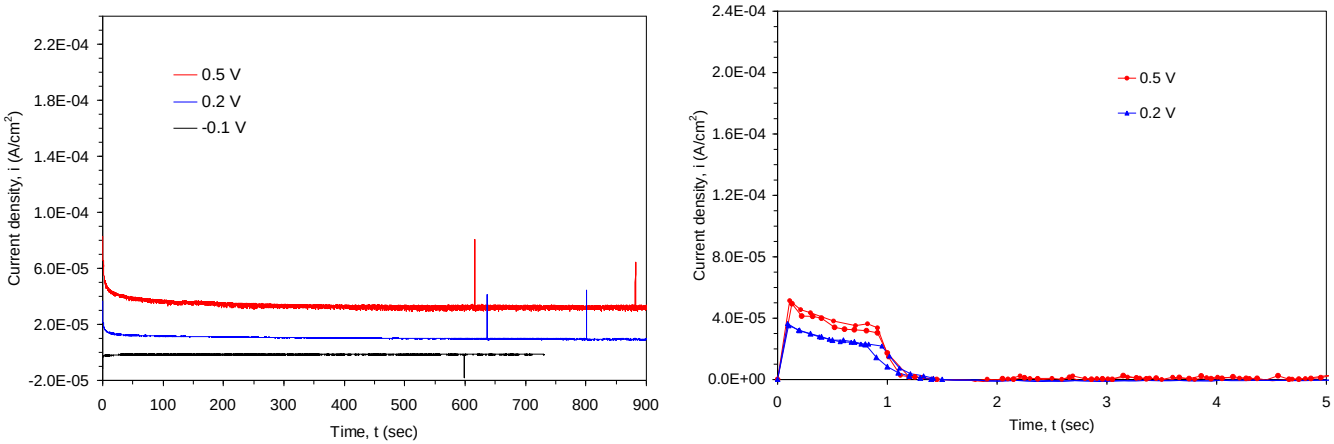

(a) **(b)**

Figure 4: Potentiostatic polarization curves (a) and corrected current versus time transient curves (b) at various potentials in 0.5 M NaCl solution with 0.1 M Na_2S at 22 °C

The ratios of peak current with and without sulfur ranged from 0.37 to 0.40 depending on the applied potential (see Table 3). These low ratio values suggest a decrease in the film thickness when exposed in the solution containing 0.1 M Na_2S. Using Eq. (2) and the same values of parameters used in cases without sulfur, the calculated thickness of the passive film ranged from 1.25 nm at 0.2 V_{SCE} to 1.63 nm at 0.5 V_{SCE}. The addition of sulfur up to 0.1 M Na_2S did not prevent a strong tendency toward repassivation characteristics of this alloy.

This high repassivation capability of UNS N06022 indicates that this alloy may not be susceptible to localized corrosion (i.e., pitting corrosion) due to sulfur segregation. Alloying elements such as chromium and molybdenum in this alloy may play a significant role in eliminating any potential detrimental effect of sulfur segregation. The beneficial role of these alloying elements on the resistance against localized corrosion of nickel-based alloys has been generally recognized. For example, the chromium in Ni−xCr−10Fe alloys (x = 8, 19, and 34 at%) counteracts the detrimental effects of sulfur by promoting alloy passivation, whereas the passivation is precluded by sulfur in Ni or Ni−Fe alloys (no chromium) under similar conditions.[12,13,23] Addition of molybdenum in the alloys also counteracts detrimental effects of sulfur in many passive metals. In Ni−2~6Mo and Fe-17Cr-14.5Ni-2.3Mo stainless steel, the preadsorbed sulfur on the surface decreased sharply during the dissolution of alloys by removal via soluble molybdenum–sulfide formation.[14,15] UNS N06625 (Ni−21.5Cr−9Mo−4Fe) was resistant to crevice corrosion in 1 M NaCl solution containing 0.01 M $Na_2S_2O_3$ up to 80 °C, whereas UNS N06600 (Ni−15.5Cr−8Fe), with no molybdenum in the alloy, was attacked by crevice corrosion in the same solution even at temperatures as low as 20 °C.[24] In particular, based on the experimental observations using radiotracer techniques, Marcus and Moscatelli have established a formula to represent sulfur dissolution kinetics for Ni-2 Mo alloy with preadsorbed sulfur on the alloy surface.[14] Using the formula developed by Marcus and Moscatelli, Ahn, et al. calculated the sulfur dissolution kinetics of UNS N06022.[14,25] The results indicate that any potential sulfur segregation on its surface could be eliminated quickly by the dissolution of the metal matrix.

Therefore, it is reasonably expected that a relatively high concentration of molybdenum in this alloy (~13 percent in weight) can effectively remove any segregated sulfur on the surface, if it was to occur. This postulate is further supported by the thermodynamic stability of UNS N06022 in sulfur-containing water systems. Jung, et al. constructed potential-pH diagrams of nickel−sulfur−water, chromium−sulfur−water, and molybdenum−sulfur−water systems at 25 and 90 ˚C for 10^{-6} M concentrations of ions in the solution.[6] The thermodynamic calculations indicate that chromium oxide

(i.e., Cr_2O_3) could be stable in a wide range of solution pHs and potentials, and a formation of possibly soluble molybdenum sulfides was also predicted.

Effect of Aeration

The effect of aeration on the repassivation behavior of UNS N06022 was investigated under a sulfur-contaminated condition. Figure 5 presents the current versus time transient curves polarized at 0.2 and 0.5 V_{SCE} in aerated 0.5 M NaCl solution containing 0.01 M Na_2S at 22 °C. The curves for the deaerated condition are also presented for comparison in the same figure.

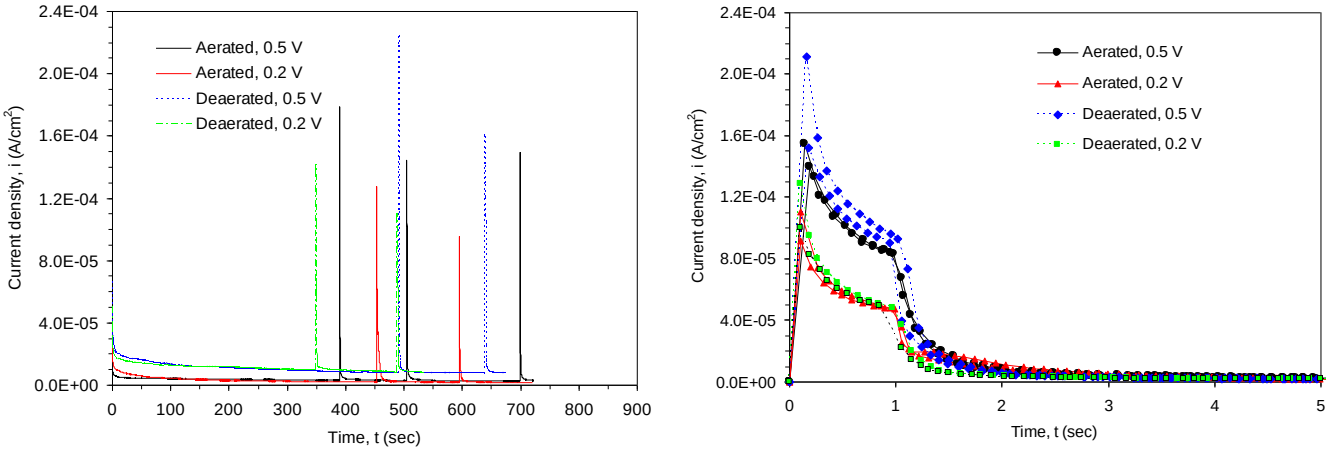

(a) **(b)**

Figure 5: Potentiostatic polarization curves (a) and corrected current versus time transient curves (b) at 0.2 and 0.5 V_{SCE} in Aerated 0.5 M NaCl Solutions Containing 0.01 M Na_2S in Comparison With Deaerated Conditions at 22 °C.

In the figure, aeration did not noticeably influence the peak current and repassivation rate of UNS N06022. This is most likely because the electron-generating reactions (i.e., metal dissolution and oxide repassivation via water hydrolysis) are not appreciably influenced by the presence of dissolved oxygen during the repassivation process at the scratched area. The results of the aeration effects on repassivation of UNS N06022 were applicable to simulated concentrated water in an aerated condition.

Repassivation in Aerated Simulated Concentrated Water

The current transient versus time curves of UNS N06022 in aerated simulated concentrated water containing 0.01 M Na_2S are presented in Figure 6. In this solution, the alloy samples repassivated within ~2 seconds after the scratch. This rapid repassivation in aerated simulated concentrated water shares a trend with the aerated 0.5 M NaCl solution in which both solutions contain 0.01 M Na_2S at 22 °C. As seen in the figure, however, the peak current decreased in simulated concentrated water, suggesting a decrease of reformed film thickness, or alteration of the chemical kinetics.

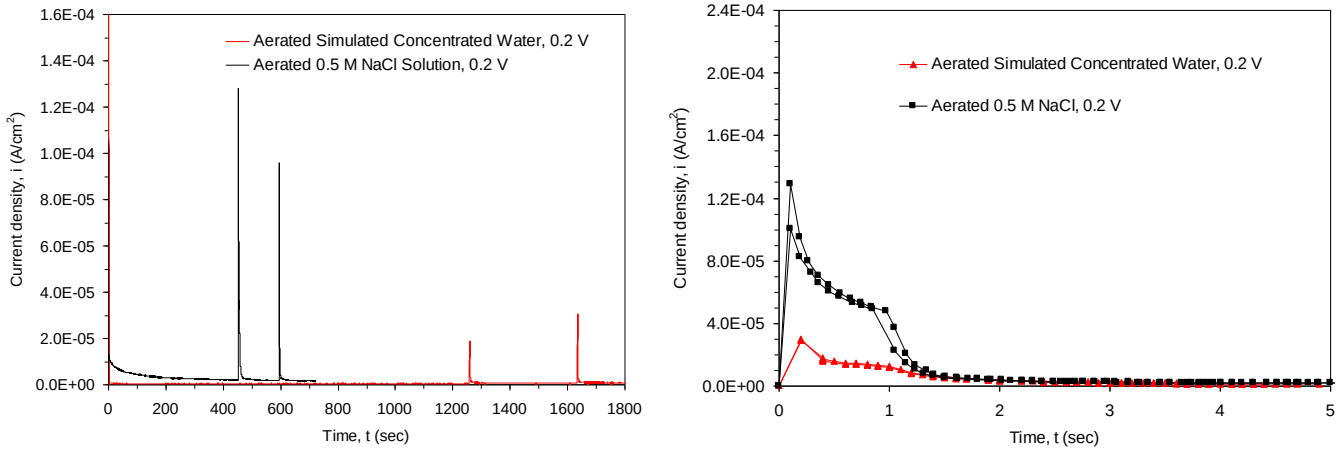

(a) **(b)**

Figure 6: Potentiostatic polarization curves (a) and corrected current versus time transient curves (b) at 0.2 V_{SCE} in aerated simulated concentrated water containing 0.01 M Na_2S in comparison with the potentiostatic polarization curve in aerated 0.5 M NaCl solution containing 0.01 M Na_2S at 22 °C.

Considering high concentrations of oxyanions (i.e., nitrates, sulfate, and carbonates) in simulated concentrated water (see Table 2), an apparent decrease in film thickness could be due to a higher chloride concentration in simulated concentrated water (1.89 M Cl^-), leading to a faster dissolution rate of this alloy . These oxyanions have been known as effective inhibitors for the localized corrosion of this alloy in a binary solution of 0.5 m NaCl at 95 °C, while chloride has an opposite role by initiating and promoting localized corrosion.[2] Even if there are some uncertainties associated with different solution pHs (i.e., pH of 7 for 0.5 M NaCl and pH of ~10 for simulated concentrated water), a relatively high concentration of chloride content in simulated concentrated water might play a more significant role by counteracting the effect of oxyanions during the repassivation process. Nonetheless, UNS N06022 repassivates within a few seconds when the passive film is mechanically disrupted in simulated concentrated water containing 0.01 M Na_2S at 22 °C.

Repassivation Behavior of UNS N06022 at 60 °C

To explore the effect of solution temperature on the repassivation behavior of UNS N06022 in sulphur-containing conditions, scratch repassivation tests were conducted at 60 °C. The resultant responses with and without 0.01 M Na_2S are presented in Figures 7 and 8, respectively. The values of corrected peak currents are listed in Table 4.

Table 4
Peak Current Density Measured at −0.1, 0.2, and 0.5 V_{SCE} in 0.5 M NaCl Solution Without and with 0.01 M Na_2S at 60 °C

Potential (V_{SCE})	Corrected i_{peak} (A/cm^2)				
	Without Sulfur		0.01 M Na_2S		Average Ratio (0.01M Sulfur Versus Without Sulfur)
	Peak #1	Peak #2	Peak #1	Peak #2	
−0.1	7.64×10^{-5}	7.38×10^{-5}	5.14×10^{-5}	4.91×10^{-5}	0.67
0.2	1.71×10^{-4}	1.48×10^{-4}	6.92×10^{-5}	7.34×10^{-5}	0.45
0.5	2.52×10^{-4}	2.21×10^{-4}	8.66×10^{-5}	7.73×10^{-5}	0.35

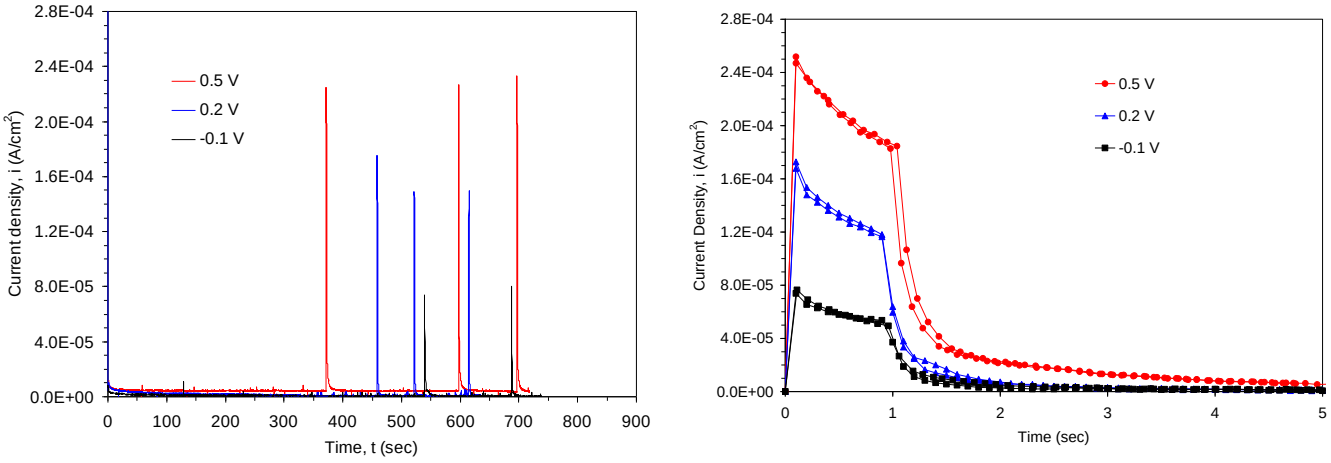

(a) **(b)**

Figure 7: Potentiostatic polarization curves (a) and corrected current versus time transient curves (b) at various potentials in 0.5 M NaCl solution without sulfur at 60 °C.

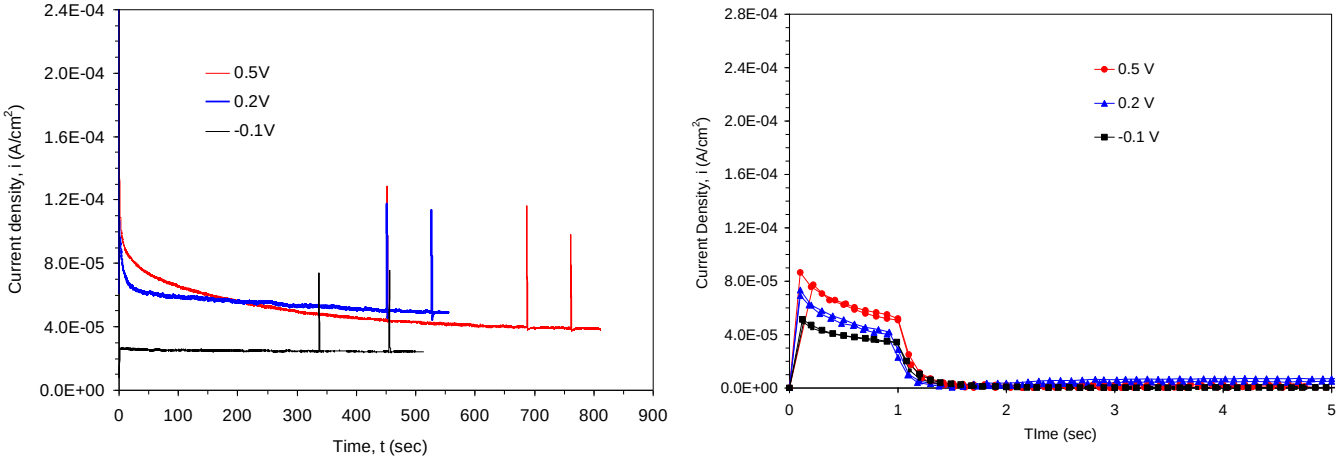

(a) **(b)**

Figure 8: Potentiostatic polarization curves (a) and corrected current versus time transient curves (b) at various potentials in 0.5 M NaCl solution containing 0.01 M Na_2S at 60 °C.

For cases with and without sulfur, the test alloys repassivated within a few seconds after scratching. However, the average ratio of peak current from a sulfur-containing solution to a solution without sulfur was less than one and decreased as the potential increased. The average ratios at 60 °C are 0.67, 0.45, and 0.35 at −0.1, 0.2, and 0.5 V_{SCE}, respectively. The average ratio of one was observed at 22 °C at the same concentration of Na_2S addition (i.e., 0.01 M). Moreover, the peak currents are slightly lower than those at 22 °C. These results may suggest that sulfur leads to a smaller film thickness on the alloy as the temperature increases. This alloy was, however, still able to passivate within a few seconds, and no active dissolution occurred at the scratched surface area at 60 °C.

CONCLUSIONS

Based on the experimental data of the scratch repassivation test and calculations on the reformed film thickness of UNS N06022, several conclusions can be drawn.

- For all UNS N06022 samples tested in chloride-containing solutions with and without sulfur content at 22 and 60 ˚C, once a passive film was mechanically disrupted by scratching, the anodic current increased abruptly to a peak value and thereafter decreased toward a steady-state value within a few seconds, implying a strong repassivation tendency of UNS N06022.

- In the absence of sulfur, the peak current increased proportionally as the anodic potential increased from −0.1 to 0.5 V_{SCE}. Assuming a mixture of chromium oxide and nickel oxide of the reformed passive film, the thickness of the oxide film was inferred to increase from 1.8 nm at −0.1 V_{SCE} to 2.7 nm at 0.5 V_{SCE}, which is consistent with the literature data.

- Addition of sulfur in a concentration of 0.01 M Na_2S tested at 22 °C did not result in an enhanced corrosion rate, and the repassivation capability of the alloy did not deteriorate.

- The addition of sulfur up to 0.1 M Na_2S or increase of test temperature up to 60 °C, however, resulted in a decrease of peak current, suggesting a decrease of passive film thickness. Nevertheless, the alloy showed a strong tendency toward repassivation.

- Aeration did not noticeably influence the peak current and repassivation rate of UNS N06022. In an aerated simulated concentrated water containing sulfur, the peak current decreased; the alloy still repassivated within a few seconds.

- It is likely that chromium and molybdenum in UNS N06022 are mostly responsible for the high repassivation capability by counteracting any potential detrimental effects of adsorbed sulfur on the alloy surface.

ACKNOWLEDGMENTS

The authors gratefully acknowledge the reviews of Drs. O. Pensado and S. Mohanty, the editorial review of L. Mulverhill, and the assistance of J. Gonzalez and J. Simpson in the preparation of this manuscript.

DISCLAIMER

This paper is an independent product of Center for Nuclear Waste Regulatory Analyses[1] and does not necessarily reflect the view or regulatory position of U.S. Nuclear Regulatory Commission[2]. The Nuclear Regulatory Commission staff views expressed herein are preliminary and do not constitute a final judgment or determination of the matters addressed or of any licensing action that may be under consideration at Nuclear Regulatory Commission.

REFERENCES

1. M. Fontana, *Corrosion Engineering*, 3rd Edition. Singapore: McGraw-Hill. 1987.

2. D.S. Dunn, O. Pensado, Y.-M. Pan, R.T. Pabalan, L. Yang, X. He, and K.T. Chiang, “Passive and Localized Corrosion of Alloy 22—Modeling and Experiments.” CNWRA 2005-02. Rev. 1. San Antonio,

[1] Center for Nuclear Waste Regulatory Analyses, 6220 Culebra Road, San Antonio, TX 78238
[2] U.S. Nuclear Regulatory Commission, MS E2–B2, Washington, DC 20555-0001

Texas: CNWRA. 2005.

3. O. Pensado, D.S. Dunn, G.A. Cragnolino, and V. Jain, “Passive Dissolution of Container Materials—Modeling and Experiments.” CNWRA 2003-01. San Antonio, Texas: CNWRA. 2002.

4. K.T. Chiang, D.S. Dunn, Y.-M. Pan, O. Pensado, and P.K. Shukla, “Stress Corrosion Cracking of Waste Package Material—Modeling and Experiments.” CNWRA 2007-01. San Antonio, Texas: CNWRA. 2007.

5. A.C Lloyd, J.J. Noël, S. McIntyre, and D.W. Shoesmith, “Cr, Mo and W Alloying Additions in Ni and Their Effect on Passivity.” *Electrochimica Acta*. Vol. 49. pp. 3,015–3,027. 2004.

6. H. Jung, T. Mintz, D.S. Dunn, O. Pensado, and T. Ahn, “A Review of the Long-Term Persistence of the Passive Film on Alloy 22 in Potential Yucca Mountain Repository Environments.” ML072880595. Washington, DC: NRC. 2007. <www.nrc.gov/reading-rm/adams.html> (5 March 2008).

7. P. Marcus, H. Talah, and J. Oudar, “Breakdown of the Passive Film on Nickel and Nickel Alloys Induced by Sulfur.” *Key Engineering Materials*. Vols. 20–28, Issue 4. pp. 3,947–3,952. 1988.

8. P. Marcus, J. Oudar, and I. Olefjord, “Studies of the Influence of Sulfur on the Passivation of Nickel by Auger Electron Spectroscopy and Electron Spectroscopy for Chemical Analysis.” *Materials Science and Engineering*. Vol. 42. pp. 191–197. 1980.

9. J. Oudar, and P. Marcus, “Roles of Adsorbed Sulphur in the Dissolution and Passivation of Nickel and Nickel-Sulphur Alloys.” *Application of Surface Science*. Vol. 3. pp. 48–67. 1979.

10. P. Marcus, A. Testier, and J. Oudar, “The Influence of Sulphur on the Dissolution and the Passivation of a Nickel-Iron Alloy—Electrochemical and Radiotracer Measurements.” *Corrosion Science*. Vol. 24, No. 4. pp. 259–268. 1984.

11. P. Marcus, I. Olefjord, and J. Oudar, “The Influence of Sulfur on the Dissolution and the Passivation of a Nickel-Iron Alloy—Sulfur Analysis by ESCA.” *Corrosion Science*. Vol. 24, No. 4. pp. 269–278. 1984.

12. D. Costa and P. Marcus, “Modification of Passive Films Formed on Ni-Cr-Fe Alloys With Chromium Content in the Alloy and Effects of Adsorbed or Segregated Sulphur.” Proceedings of the European Symposium on Modifications of Passive Film, Paris, France, February 15–17, 1993. pp. 17–25. 1993.

13. P. Marcus and J.M. Grimal, “The Antagonistic Roles of Chromium and Sulfur in the Passivation of Ni-Cr-Fe Alloys Studies by XPS and Radiochemical Techniques.” *Corrosion Science*. Vol. 31. pp. 377–382. 1990.

14. P. Marcus and M. Moscatelli, “The Role of Alloyed Molybdenum in the Dissolution and the Passivation of Nickel-Molybdenum Alloys in the Presence of Adsorbed Sulfur.” *Journal of the Electrochemical Society*. Vol. 136, No. 6. pp. 1,634–1,637. 1989.

15. A. Elibiache and P. Marcus, “The Role of Molybdenum in the Dissolution and the Passivation of Stainless Steels With Adsorbed Sulphur.” *Corrosion Science*. Vol. 33, No. 2. pp. 261–269. 1992.

16. G.T. Burstein and P.I. Marshall, “Growth of Passivating Films on Scratched 304L Stainless Steel in Alkaline Solution.” *Corrosion Science*. Vol. 23, No. 4. pp. 125–137. 1983.

17. H.C. Brookes, J.W. Bayles, and F.J. Graham, “Nucleation and Growth of Anodic Films on Stainless Steel Alloys. I. Influence of Minor Alloying Elements and Applied Potential on Passive Film Growth.”

Journal of Applied Electrochemistry. Vol. 20. pp. 223–230. 1990.

18. R.C Newman, "The Dissolution and Passivation Kinetics of Stainless Alloys Containing Molybdenum—I. Coulometric Studies of Fe-Cr and Fe-Cr-Mo Alloys." *Corrosion Science*. Vol. 25, No. 5. pp. 331–339. 1985.

19. J.L. Gilbert, C.A. Buckley, and E.P. Lautenschlager, "Titanium Oxide Film Fracture and Repassivation: The Effect of Potential, pH and Aeration." *Medical Applications of Titanium and Its Alloys*. S.A. Brown and J.E. Lemons, eds. *STP 1272*. West Conshohocken, Pennsylvania: ASTM International. 1996.

20. D.R. Lide, ed., *Handbook of Chemistry and Physics*. 72nd Edition. Boston, Massachusetts: Chemical Rubber Corporation, CRC Press. pp. 4–36. 1992.

21. A.C. Lloyd, D.W. Shoesmith, N.S. McIntyre, and J.J. Noël, "Effects of Temperature and Potential on the Passive Corrosion Properties of Alloys C22 and C276." *Journal of the Electrochemical Society*. Vol. 150. pp. B120–B130. 2003.

22. R. Kircheim, "Growth Kinetics of Passive Films." *Electrochimica Acta*. Vol. 32. pp. 1,619–1,629. 1987.

23. P. Combrade, P. Marcus, and A. Gelpi, "Effect of Sulfur on the Protective Layers on Alloys 600 and 690 in Low and High Temperature Environments." Proceedings of the Fourth International Symposium on Environmental Degradation of Materials in Nuclear Power Systems—Water Reactors, Jekyll Island, Georgia, August 6–10, 1989. D. Cubicciotti, ed. Houston, Texas: NACE International. pp. 429–442. 1990.

24. S.J. Mulford and D. Tromans, "Crevice Corrosion of Nickel-Based Alloys in Neutral Chloride and Thiosulfate Solutions." *Corrosion*. Vol. 44, No. 12. pp. 891–900. 1988.

25. T. Ahn, H. Jung, X. He, and O. Pensado, "Understanding Long-Term Corrosion of Alloy 22 Container in the Potential Yucca Mountain Repository for High-Level Nuclear Waste Disposal." *Journal of Nuclear Materials.* Vol. 379. pp. 33-41. 2008.